RESEARCH SERIES.

Machine Learning Stacking Ensemble for Condition Assessment of Power Cable Networks

Mohsen Mohammadagha[1✉*], Atena Khoshkonesh[1], Shayan Sharifi[2], Amir Ali Belbasi[1], Vahid Ghanbarizadeh[3], Saeid Ataei[4], Kooshyar Lahsaei[1], Mohammad Sarajzadeh[1]

[1] UNIVERSITY OF TEXAS AT ARLINGTON

[2] WAYNE STATE UNIVERSITY

[3] FLORIDA ATLANTIC UNIVERSITY

[4] STEVENS INSTITUTE OF TECHNOLOGY

Abstract: Underground 15-kV XLPE cable networks are critical to distribution reliability yet degrade through aging, partial discharge (PD), and corrosion, motivating data-driven condition assessment beyond periodic manual inspection. This study addresses the need for scalable and explainable models on real utility inspection records by developing an interpretable multi-model stacking ensemble to classify categorical visual condition states. Using 2,500 asset-level cable records from Western Canada, four standardized predictors (Age, Partial_Discharge, Neutral_Corrosion, Loading) were analyzed and modeled with Logistic Regression, Gradient Boosting, Random Forest, and a stacking ensemble with a Random Forest meta-learner. The stacking ensemble achieved the best overall performance, with accuracy 95.80%, precision 95.79%, recall 95.80%, and F1-score 95.72%, while feature-importance and SHAP-based explanations consistently identified Age and PD as dominant degradation drivers. Future work should validate transferability across multiple utilities, incorporate temporal PD/loading trajectories, quantify uncertainty and drift for deployment, and integrate model outputs into EAM/GIS workflows for operational decision support.

Keywords: *Machine Learning, Ensemble Method, Condition Assessment, Underground Infrastructure.*

✉ **Corresponding author**
Mohsen Mohammadagha
University of Texas at Arlington
701 S. Nedderman Drive
Arlington, Texas, 76019,
USA.
Email: mxm4340@mavs.uta.edu
Orcid: 0009-0007-0394-353X

[1✉*] Ph.D. Candidate at Department of Civil Engineering, University of Texas at Arlington, Arlington, Texas, USA. Correspondence: mxm4340@mavs.uta.edu (M.M)

1 INTRODUCTION

The reliable operation of urban power distribution networks is fundamentally dependent on the health and resilience of their underlying infrastructure [1], particularly underground cross-linked polyethylene (XLPE) cable systems. As cities expand and energy demands intensify, the integrity of these buried assets becomes increasingly critical for ensuring uninterrupted power delivery, public safety, and economic stability. XLPE cables [2], widely adopted for their superior insulation and longevity, are nonetheless susceptible to deterioration due to environmental factors, electrical stresses, and aging. Traditional inspection [3] and maintenance approaches, often reliant on periodic manual assessments, are resource-intensive and may fail to capture the nuanced, evolving risks [4] inherent in large-scale cable networks [5]. This context underscores the need for advanced, data-driven methodologies [6][7] that can provide timely, accurate, and actionable insights into infrastructure condition, thereby enabling smarter asset management [8][9] and risk mitigation strategies [10][11][12].

Recent advances in machine learning (ML) [13] have opened new avenues for infrastructure condition assessment, offering the potential to extract meaningful patterns from complex, high-dimensional datasets [14] that characterize cable health [15]. The application of ML techniques to power asset management [16] is particularly promising, as it enables the integration of diverse condition attributes [17]—such as partial discharge, neutral corrosion, and visual inspection results—into predictive models that can forecast degradation and prioritize interventions [18]. However, the heterogeneity of real-world data and computational models [19][20][21][22] and the multifaceted nature of cable aging processes present analytical challenges. Addressing these requires not only robust feature engineering [23][24] and model selection but also the adoption of ensemble learning frameworks that can leverage the strengths of multiple algorithms to enhance predictive accuracy and reliability [25].

In this study, we address the challenge of assessing underground power cable infrastructure through advanced machine learning methodologies [26][27] applied to utility-maintained inspection records spanning multiple decades. The analytical framework [28][29] leverages normalized [30][31] diagnostic indicators, including partial discharge signatures, corrosion progression metrics, visual condition assessments, and operational loading profiles, which collectively capture the complex interplay of physical [32][33][34][35], electrical, and environmental degradation mechanisms affecting cable longevity. These multidimensional condition attributes provide a robust foundation for developing predictive models that can quantify infrastructure health trajectories. The primary objective is to establish and validate a multi-model ensemble framework [36] that integrates classical machine-learning algorithms—including logistic regression [37], gradient-boosting methods [38], and random-forest classifiers [39][40]—to advance condition-based asset management practices for critical underground distribution networks [41].

In summary, this work proposes a new approach, machine learning-based methodology for the condition assessment of underground XLPE cable networks, emphasizing the use of multi-model ensembles to address the inherent complexity and uncertainty of infrastructure health data. The approach is designed to advance the state of the art in predictive maintenance and asset management for power utilities, offering both methodological innovation and practical relevance. The subsequent sections of this article will detail the related literature, methodological framework, empirical results, discussion of findings, and recommendations for future research and industry application.

2 RELATED WORKS

The advancement of cable diagnostics and condition assessment [42] has been propelled by the integration of artificial intelligence, advanced sensing, and novel analytical techniques. Recent research has focused on enhancing the accuracy, speed, and reliability of detecting and classifying faults and degradations in power cables, particularly those insulated with cross-linked polyethylene (XLPE). These studies collectively demonstrate a shift towards data-driven and non-destructive methodologies, leveraging both simulated and experimental datasets to validate new approaches. The comparative analysis of these works reveals the breadth of strategies, from neural network-based diagnostics to evolved gas analysis and hybrid feature extraction, each contributing unique strengths to the field of cable monitoring [43] and predictive maintenance.

A notable comparison can be drawn between the works of Boukezzi and Boubakeur (2013) and Huo et al. (2020), both of which utilize neural networks for cable diagnostics but differ in their methodologies and datasets. Boukezzi and Boubakeur employed supervised and unsupervised neural networks, including Radial Basis Function (RBF) networks trained by Back-Propagation and Random Optimization Method (ROM), to predict the mechanical properties of XLPE cable insulation under thermal aging. Their experimental dataset comprised 320 samples aged at various temperatures and durations, with the ROM-trained RBF achieving maximum relative errors of 14.8% for elongation and 5.1% for tensile strength [44]. In contrast, Huo et al. generated large synthetic datasets simulating water-tree degradation in medium-voltage XLPE cables, using feed-forward neural networks (FFNNs) to sequentially detect, classify, and locate degradations. Their models were trained on tens of thousands of samples, achieving competitive accuracy relative to prior work, and required no manual feature extraction. While Boukezzi & Boubakeur's approach was validated on real experimental data with accuracy, Huo et al.'s method demonstrated scalability and automation potential using only end-to-end channel data, highlighting the evolution from laboratory-based to fully automated diagnostics [45].

Comparing the reviews by Kumar et al. (2024) and Li et al. (2023) illustrates the diversity of diagnostic techniques and the increasing role of artificial intelligence in cable health monitoring. Kumar et al. provided an extensive survey of partial discharge (PD) classification in medium-voltage cables, emphasizing feature extraction across time, frequency, and wavelet domains, and the application of AI-based classifiers such as support vector machines and deep learning. Their review reported classification accuracies up to 99.82% for convolutional neural networks and 97% PD signal separation using cross wavelet transform, underscoring the effectiveness of AI in PD diagnostics [46]. Li et al., on the other hand, focused on condition monitoring and defect inspection for composited cable terminals, analyzing both online and offline diagnostic methods, including partial discharge, UHF, ultrasonic, and terahertz techniques. They highlighted a PD-based defect classification accuracy of 96% and successful terahertz detection of air-gap defects in XLPE samples. While both reviews underscore the importance of non-destructive and AI-driven approaches, Kumar et al. stress the superiority of deep learning for PD classification, whereas Li et al. advocate for multi-source information fusion and digital twin technologies as future directions [47].

Highlighting the application of advanced feature extraction and non-electrical diagnostics, the works of Said et al. (2022) and Kong et al. (2023) offer contrasting approaches to fault classification. Said et al. developed a deep learning-based method for fault classification and location in 11kV underground cable facilities, utilizing a simulated dataset of 9405 samples generated via ATP/EMTP. Their methodology combined Fractional Discrete Cosine Transform (FrDCT) and Singular Value Decomposition (SVD) for feature extraction, Binary Support

Vector Machine (BSVM) for detection, and a 1D Convolutional Neural Network (1D-CNN) for classification and location, achieving 99.6% classification accuracy and a maximum location error of 0.095% [48]. Kong et al. introduced a novel condition assessment technique for high-voltage corrugated aluminum sheathed XLPE cables based on evolved gas analysis (EGA), using thermogravimetric and mass spectrometric analyses to characterize gases generated during faults. Their experimental dataset included pyrolysis and discharge-induced degradation results, with field validation on 220 kV cables. Notably, high-energy discharges produced large amounts of CO2 and other chemicals, with electrochemical corrosion yielding H2 concentrations over 20,000 ppm. While Said et al. demonstrated the power of deep learning and hybrid feature extraction for real-time diagnostics, Kong et al. provided a sensitive, non-destructive alternative through gas analysis, expanding the toolkit for comprehensive cable health assessment [49].

In summary, the reviewed literature demonstrates a trend towards integrating artificial intelligence [50], advanced sensing [51], and multi-modal data analysis for cable diagnostics and condition assessment [52]. The comparative analyses reveal that while neural networks and deep learning approaches [53] offer high accuracy and scalability, non-destructive techniques such as evolved gas analysis and terahertz imaging provide complementary benefits, particularly for early fault detection and real-time monitoring. The diversity of datasets—from controlled laboratory experiments to large-scale synthetic simulations and field validations—ensures that these methodologies are robust and adaptable to a wide range of cable types and operational environments. Collectively, these works underscore the necessity of hybrid, noise-tolerant, and automated solutions for the future of reliable and efficient power cable diagnostics. However, despite growing adoption of ensemble learning in related power-asset diagnostics, comparatively fewer studies have applied multi-model stacking ensembles to highly imbalanced, tabular, asset-level field-inspection records for underground cable condition classification. This study addresses that underexplored setting by combining logistic regression, gradient boosting, and random forest learners within a stacking framework to predict the visual condition of 15-kV XLPE cable segments.

3 METHODOLOGY

The proposed multi-model ensemble framework commenced with systematic data acquisition from a utility-maintained repository comprising 2,500 underground 15-kV XLPE cable [54] segments asset inspection across Western Canada between 2003 and 2018. Raw inspection records captured five critical condition parameters: chronological age (years), normalized partial discharge indices, neutral corrosion severity, peak loading profiles, and categorical visual condition assessments. Following initial data ingestion, preprocessing protocols addressed data integrity through missing value imputation, outlier detection [55] via interquartile range analysis, and temporal consistency verification across multi-year inspection cycles. Statistical profiling established baseline distributions for each predictor variable by removing duplicate records to ensure dataset uniqueness. This preparatory phase provides a suitable basis for model development and training.

Feature engineering commenced with comprehensive exploratory data analysis employing Pearson correlation matrices [56] to quantify linear dependencies among condition indicators, as depicted in the Data Preparation Phase flowchart in Figure 1. Correlation coefficients revealed strong positive associations between age-partial discharge, age-neutral corrosion, and partial discharge-neutral corrosion, confirming their synergistic contribution to cable degradation mechanisms, while loading exhibited weak correlations with other parameters. Z-score normalization [57] was applied using StandardScaler according to Eq.1:

$$X_{\text{scaled}} = \frac{X - \mu}{\sigma} \tag{1}$$

Where each feature X is standardized by subtracting the mean μ and dividing by the standard deviation σ, ensuring equivalent scaling across disparate measurement units and preventing dominance by high-magnitude features during gradient-based optimization. The dataset includes a pre-computed health index (HI) composite metric (ranging from 1 = critical to 5 = excellent), which synthesizes age, partial discharge (PD), and neutral corrosion (NC) into a unified degradation indicator for operational reference; while the primary modeling target is the categorical visual condition, HI serves as a valuable auxiliary feature and visualization aid. Stratified train-test partitioning (80:20 ratio, stratified by the target class) with LabelEncoder transformation of categorical targets completed the data preparation phase.

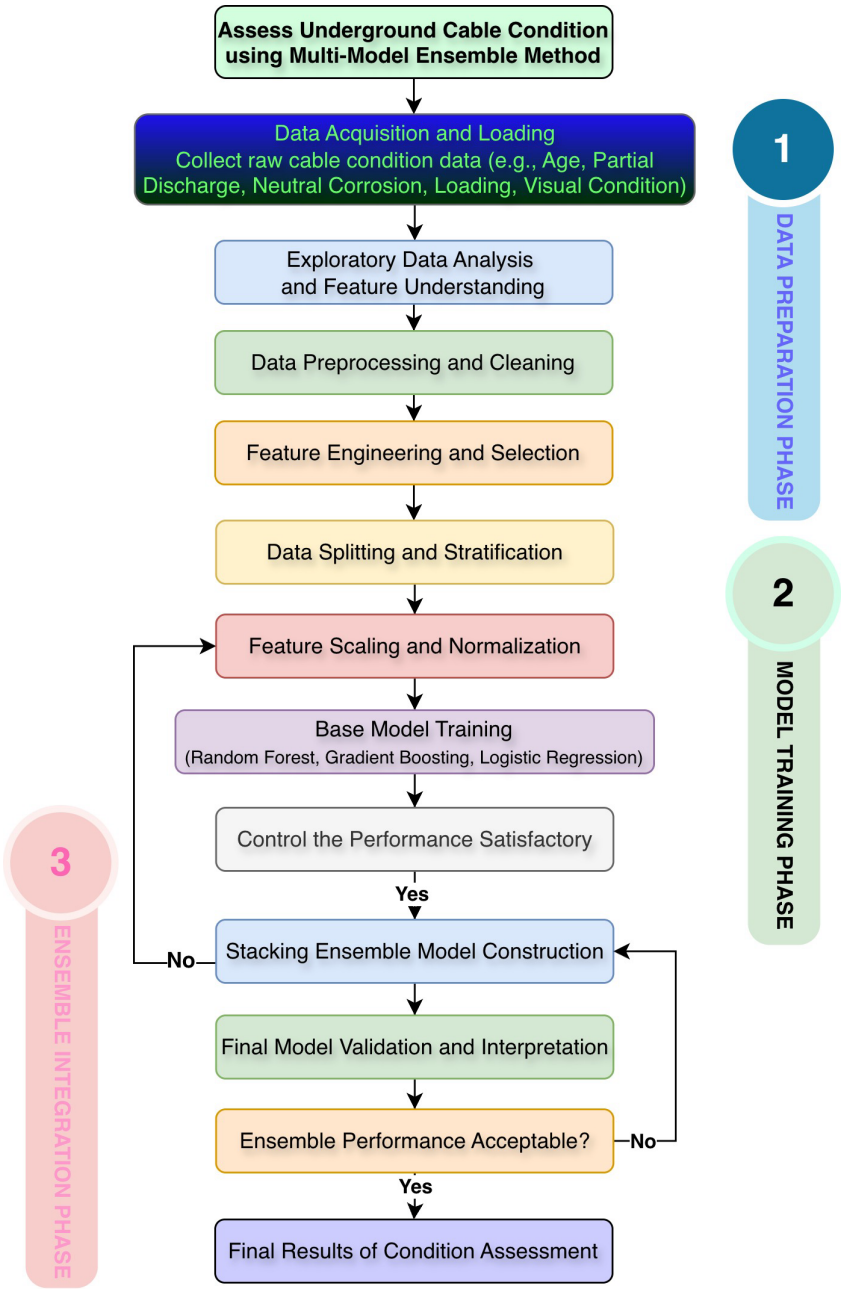

Figure 1. Stacking Ensemble Architecture for Infrastructure Assessment.

The Model Training Phase implemented three heterogeneous base learners to capture diverse degradation patterns, as illustrated in the flowchart's optimization loop. Logistic Regression served as a linear probabilistic classifier, Gradient Boosting (from scikit-learn) applied additive tree expansion with gradient descent optimization, and Random Forest classification employed the Gini impurity [58] criterion in Eq.2 at each decision node t, measuring classification purity across C condition classes with probabilities p_i.

$$Gini(t) = 1 - \sum_{i=1}^{C} p_i^2 \tag{2}$$

It constructed 1000 decision trees through bootstrap aggregation to minimize variance and enhance generalization. Each base model used default or fixed hyperparameters (n_estimators=1000 for tree-based models), with performance evaluated via five-fold cross-validation during stacking to prevent overfitting.

The Ensemble Integration Phase synthesized the optimized base learners through a stacking architecture, as delineated in the flowchart's outer validation loop. Meta-predictions [59] were generated via Eq.3:

$$y_{\text{meta}} = f_{\text{meta}}\big(f_1(\text{x}), f_2(\text{x}), f_3(\text{x})\big), \tag{3}$$

Where a Random Forest meta-learner aggregated probability distributions from the three base models (f_1 = Logistic Regression, f_2 = Gradient Boosting, f_3 = Random Forest), learning complementary strengths while mitigating individual weaknesses. Five-fold cross-validation during meta-learner training prevented information leakage. Ensemble performance was validated using classification accuracy, confusion matrices, precision-recall-F1 scores, and feature importance rankings across layers, with results compared against individual baselines.

Visualization and interpretability were integral to the methodology. Correlation matrices [60] and 3D feature visualizations [61] elucidated relationships among condition attributes and key degradation drivers. Feature importance plots were generated for each model, while SHAP (SHapley Additive exPlanations) values provided global and local explanations of predictions. For the stacking ensemble, permutation importance and meta-model behavior were analyzed to quantify contributions, ensuring transparency essential for trust in critical infrastructure applications and informed maintenance decisions.

Figure 2 presents boxplot distributions of five key features in the cable health assessment framework: Age, Partial Discharge, Neutral Corrosion, Loading, and Health Index. These visualizations reveal central tendencies, interquartile ranges, and outlier patterns, informing feature variability and the need for scaling. Age shows a median of 32 years with a wide spread (15–52 years), while Partial Discharge and Neutral Corrosion exhibit right-skewed distributions, reflecting progressive degradation in older cables. Loading displays a symmetric distribution centered around a median of 366 amperes, indicating operational consistency. The Health Index is concentrated between 2 and 4 (median = 3), confirming balanced representation across condition states and supporting robust classification. Health Index (HI) is included only for visualization and descriptive analysis and is not used as a predictor in the classification models.

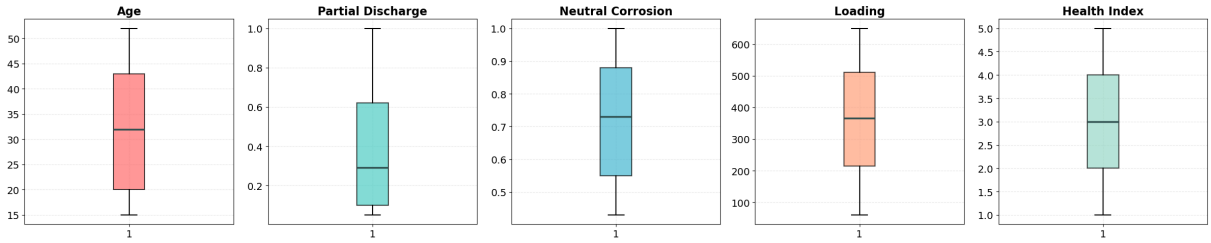

Figure 2. Boxplots of cable features for model input selection.

Table 3-1 provides comprehensive statistical summaries quantifying distributional characteristics of model input features. Cable age ranges from 15 to 52 years, with a mean of 32.21 years and a standard deviation of 12.55, reflecting diverse asset vintages. Partial Discharge spans normalized values 0.05-1.0 (mean=0.38, σ=0.31), while Neutral Corrosion exhibits higher severity (mean=0.72, σ=0.18) with a minimum of 0.43. Loading demonstrates variability (60-650 amperes, σ=169.85), and Health Index encompasses the full spectrum from critical (1) to excellent (5) with a mean of 3.14, validating balanced representation of degradation conditions for supervised classification tasks.

Table 3-1. Summary statistics of cable features.

Feature	Min	25%	Median	75%	Max	Mean	Std Dev
Age	15	20	32	43	52	32.21	12.55
Partial Discharge	0.05	0.1	0.29	0.62	1	0.38	0.31
Neutral Corrosion	0.43	0.55	0.73	0.88	1	0.72	0.18
Loading	60	214.75	366	511	650	361.66	169.85
Health Index	1	2	3	4	5	3.14	1.31

Figure 3 illustrates a pairplot of the four key numerical features—Age, Partial Discharge, Neutral Corrosion, and Loading—colored according to Health Index categories. The visualization highlights marginal distributions, bivariate relationships, and clustering tendencies that support exploratory data analysis. Strong nonlinear associations among Age, Partial Discharge, and Neutral Corrosion are visible, while Loading exhibits weaker interaction with the other indicators. These patterns provide insight into degradation behavior and inform subsequent modeling decisions within the machine-learning-based condition assessment framework.

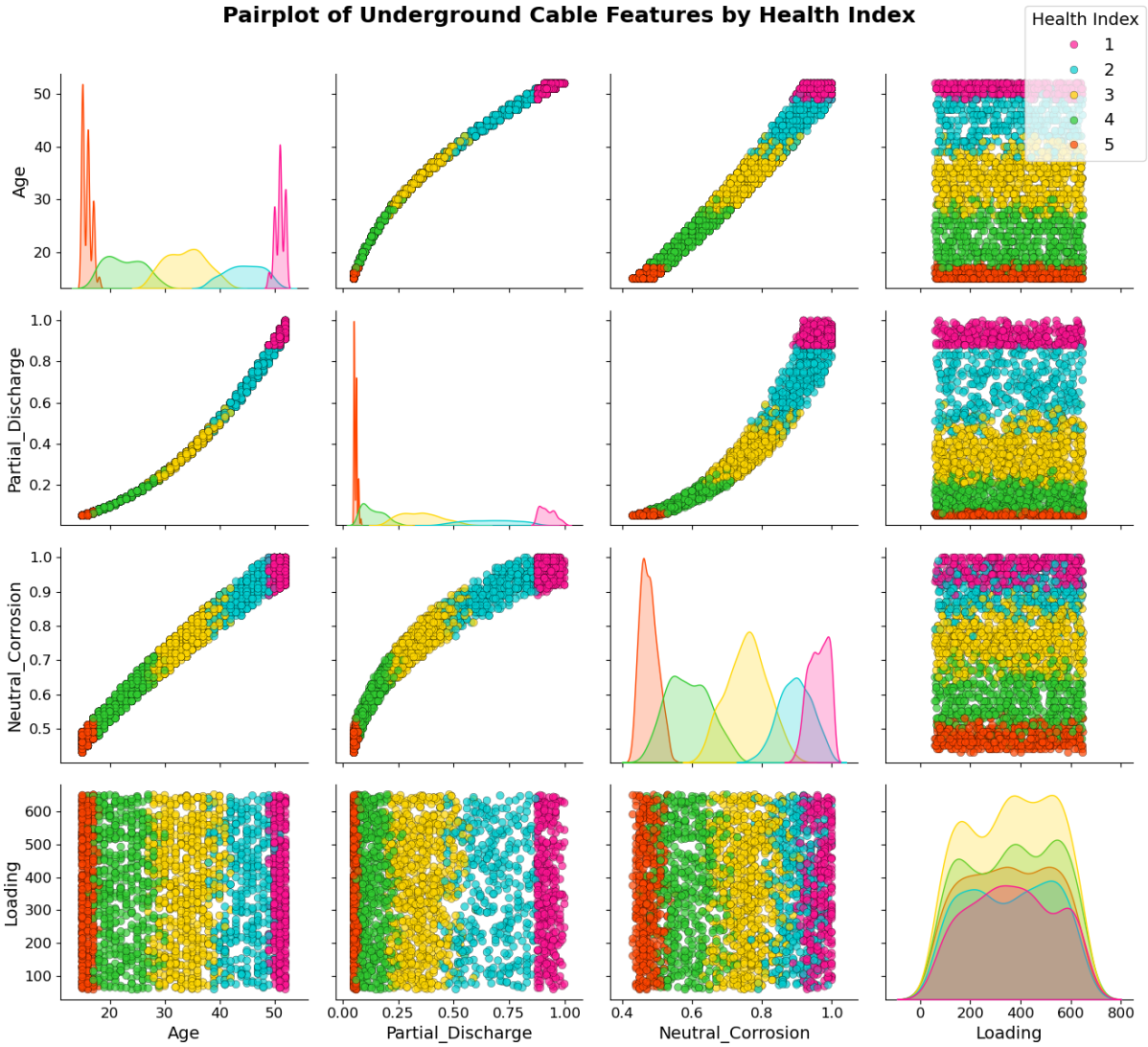

Figure 3. Pairplot of cable features colored by health index.

The Bray–Curtis PCoA plot in Figure 4 displays separation among Good, Medium, and Poor condition cables due to systematic shifts in their underlying degradation indicators into two dimensions that explain a high proportion of variance. Good cables cluster toward one region because they exhibit consistently low partial discharge and corrosion values, while Poor cables group distinctly as these indicators increase with aging. Medium cables occupy the transitional space between these extremes, reflecting moderate degradation. This pattern arises because the Bray–Curtis metric emphasizes compositional dissimilarity, causing condition groups with similar degradation profiles to cluster together.

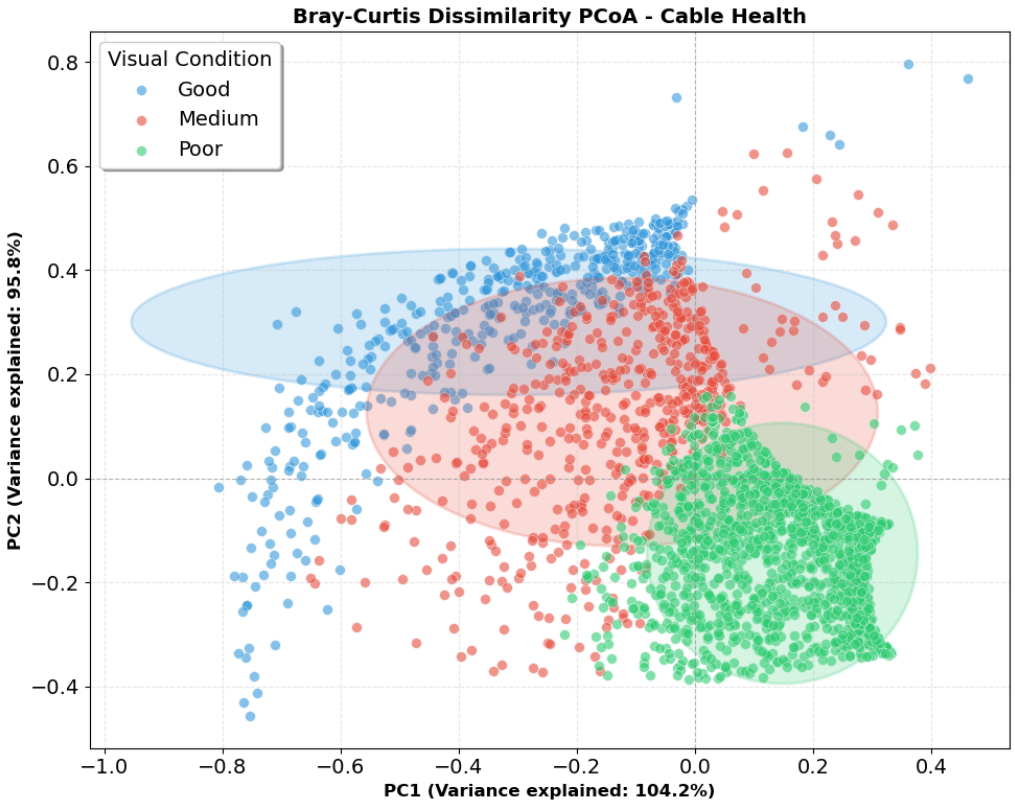

Figure 4. Bray–Curtis PCoA of cable condition groups.

Figure 5, presents a correlation heatmap illustrating the interdependencies among cable condition indicators. High positive correlations are observed between Age, Partial Discharge, and Neutral Corrosion because these elements are physically coupled, synergistically driving the progressive deterioration of XLPE insulation and metallic shields. Consequently, they align with the overall Health Index. In contrast, Loading exhibits minimal correlation with the other parameters, as the electrical current demand fluctuates independently based on operational network requirements rather than the underlying physical aging of the cable infrastructure.

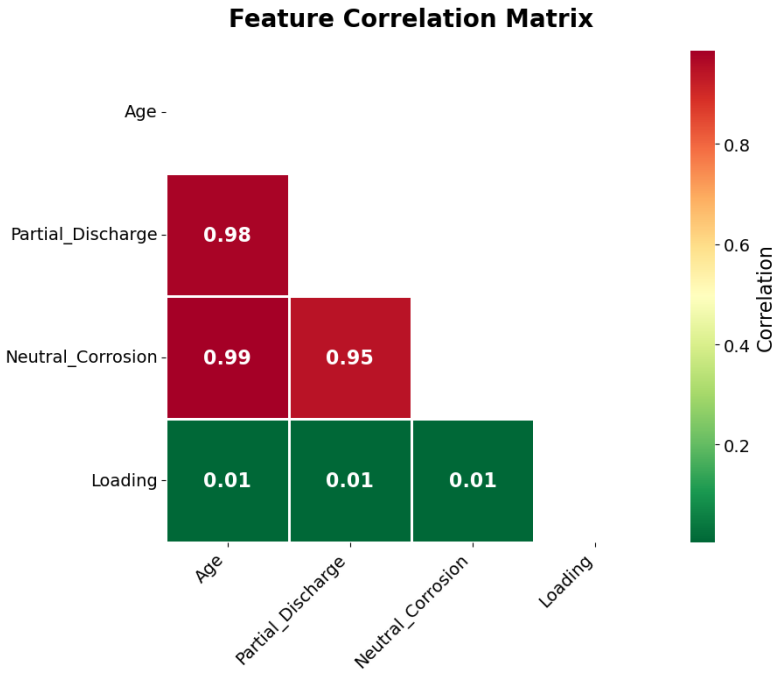

Figure 5. Pearson correlation matrix of cable condition features.

Figure 6 presents histograms of the key features (Age, Partial Discharge, Neutral Corrosion, Loading, and Health Index), with logarithmic y-scale applied to Age and Partial Discharge to better visualize skewed distributions. These plots summarize central tendencies, variability, skewness, and outliers, supporting robust exploratory analysis, feature selection, and ensuring that machine learning models are trained on well-characterized and representative data attributes.

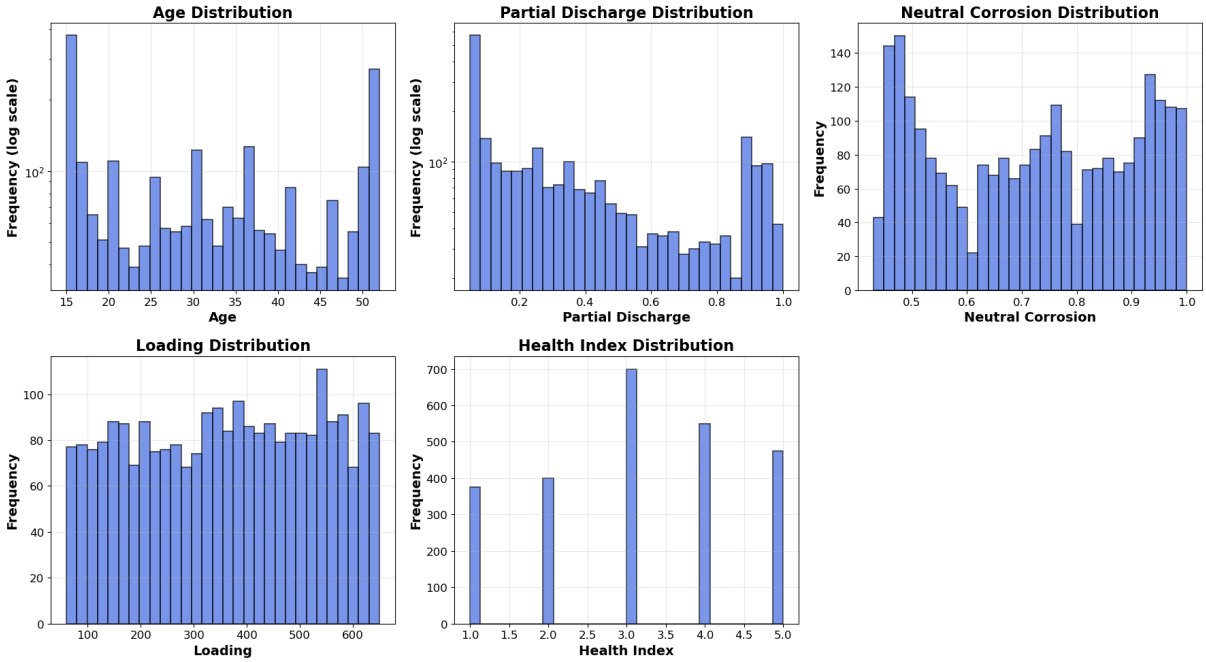

Figure 6. Distribution, central tendency, variability, and presence of outliers for each attribute.

The 3D scatter plot in Figure 7 visualizes the relationship between Age, Partial Discharge, and Neutral Corrosion, with points colored by visual condition (Good: green, Medium: yellow, Poor: pink). The distinct linear structure highlights the intercorrelations among these features, revealing a degradation pathway: as cables age and exhibit higher partial discharge and neutral corrosion, their condition deteriorates progressively from 'Good' to 'Poor'. This visualization serves as a key step in exploratory data analysis, aiding feature understanding and model interpretability.

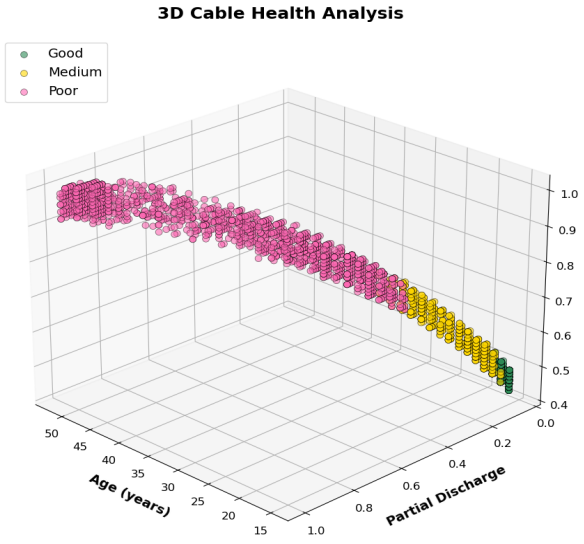

Figure 7. 3D relationships among cable age, discharge, and corrosion.

Kernel density estimation in Figure 8 visualizes the conditional age distributions across visual condition classes (Good, Medium, Poor), revealing class-specific patterns essential for understanding model discrimination capability. Good-condition cables show sharp, high-density peaks concentrated below 20 years. Medium-condition cables exhibit broader distributions with moderate density extending into mid-life ranges. Poor-condition cables display flatter, more extended densities across older ages (primarily 30–52 years), confirming age as a primary discriminative feature that supports effective multi-class classification in the ensemble framework.

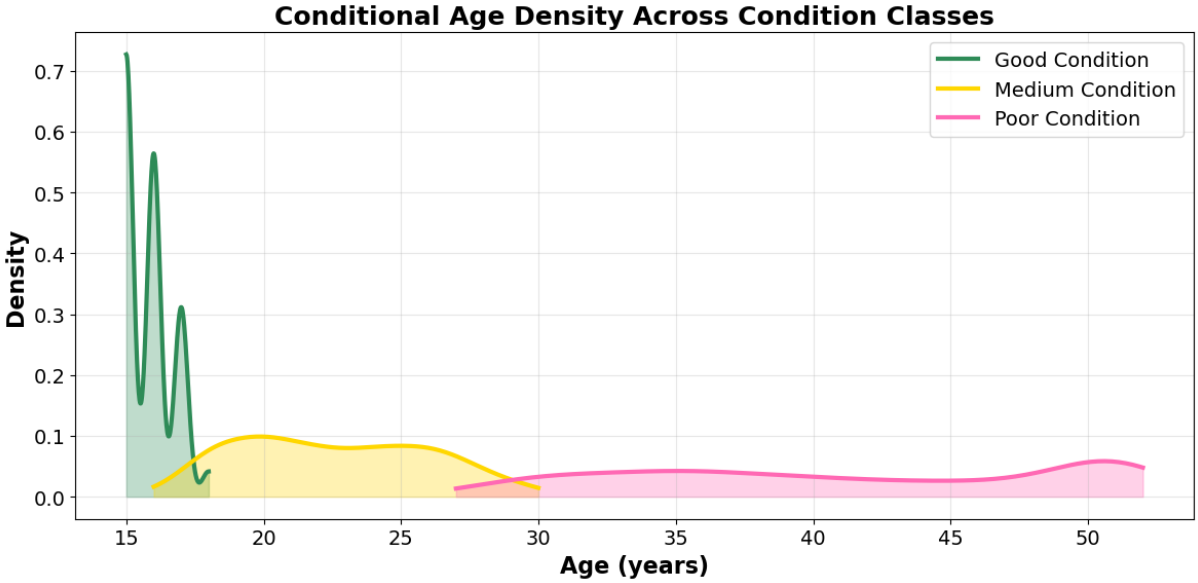

Figure 8. Conditional Age Density Across Condition Classes.

In summary, the methodology presented here fills a gap in the current literature and practice by operationalizing a multi-model stacking ensemble machine learning framework for infrastructure condition assessment, specifically tailored to underground cable networks. Unlike many prior studies that may relied on single-model approaches, laboratory-generated or simulated datasets, or limited interpretability, this work leverages a real-world, asset-level dataset, interpretable tree-based and linear models to deliver both predictive performance and actionable insights. The integration of base learners, stacking ensemble learning, and SHAP-based interpretability directly addresses the needs identified in the literature for scalable, explainable, and practical solutions in infrastructure management.

4 RESULTS

Following the methodology outlined, this section presents empirical results for the multi-model stacking ensemble applied to 2,500 15-kV XLPE cable records. The section begins with exploratory data analysis, then reports feature importance and classification performance across models, and concludes with SHAP-based interpretability to highlight key degradation drivers and ensemble effectiveness. These analyses collectively set the stage for evaluating the comparative behavior of the individual models and the stacking ensemble under consistent testing conditions.

Building on this foundation, the performance comparison in Figure 9 highlights how each classifier responds to the underlying structure of the dataset. This chart compares four classifiers using accuracy, precision, recall, and F1-score on the same test split. The stacking ensemble achieves the highest overall performance (≈95.8% accuracy), slightly outperforming logistic

regression, gradient boosting, and random forest (≈95.0–95.4%). The small gaps indicate that the feature space already separates classes well, while stacking reduces residual errors by combining complementary decision boundaries from linear and tree-based learners. The close alignment among precision, recall, and F1 suggests balanced behavior rather than a tradeoff that boosts one metric at the expense of another—important for consistent condition screening.

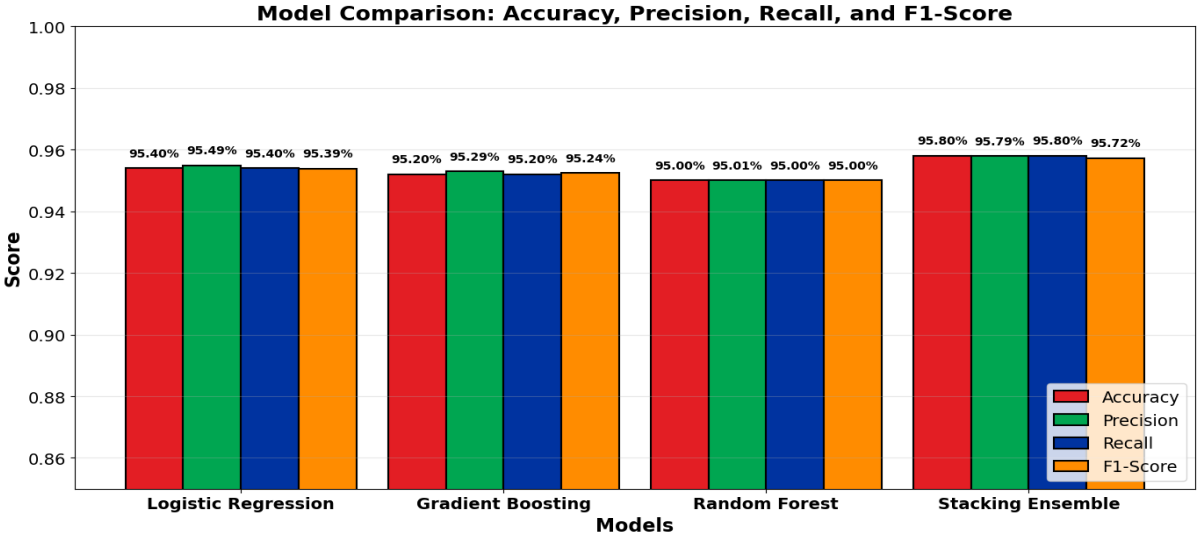

Figure 9. Model performance comparison across evaluation metrics.

Table 4-1. details precision, recall, F1-score, and support for each class across all models. The stacking ensemble achieves the highest overall accuracy (0.96) and weighted F1 (0.96), with excellent Poor-class performance (F1 = 0.98, recall = 1.00), minimizing false negatives for critical conditions. Good-class metrics remain strong (F1 ≈ 0.94), while Medium-class recall is slightly lower (0.85), reflecting the challenge of the minority class. Base models show consistently high Poor-class precision/recall (>0.98), but stacking improves Medium-class balance. These results stem from the ensemble's ability to combine tree-based robustness with linear model stability, effectively handling class imbalance and feature redundancy present in the inspection data.

Table 4-1. Class-wise precision, recall, and F1 by model

Model	Class	Precision	Recall	F1-Score	Support	Accuracy	Macro Avg F1	Weighted Avg F1
Logistic Regression	Good	0.88	0.97	0.92	95	0.95	0.93	0.95
	Medium	0.92	0.86	0.89	110			
	Poor	0.99	0.98	0.99	295			
Gradient Boosting	Good	0.93	0.93	0.93	95	0.95	0.93	0.95
	Medium	0.88	0.91	0.89	110			
	Poor	0.99	0.98	0.98	295			
Random Forest	Good	0.92	0.94	0.93	95	0.95	0.93	0.95
	Medium	0.89	0.88	0.89	110			
	Poor	0.98	0.98	0.98	295			
Stacking Ensemble	Good	0.92	0.96	0.94	95	0.96	0.94	0.96
	Medium	0.95	0.85	0.90	110			
	Poor	0.97	1.00	0.98	295			

The four-panel importance in Figure 10 shows how different learning paradigms prioritize predictors. Logistic regression allocates weight across multiple inputs, reflecting linear separation, while gradient boosting concentrates importance heavily on the strongest monotonic driver (Age), consistent with sequential tree splitting that exploits dominant gradients. Random forest distributes importance between Age and Partial Discharge, with more contribution from Neutral Corrosion and Loading, reflecting bagging and split diversity. The stacking importance (permutation-based) emphasizes Age and Partial Discharge most strongly, indicating that ensemble gains arise from jointly leveraging these drivers while reducing sensitivity to weaker, noisier predictors such as Loading. Cross-model agreement increases confidence that the learned relationships are stable rather than algorithm-specific artifacts.

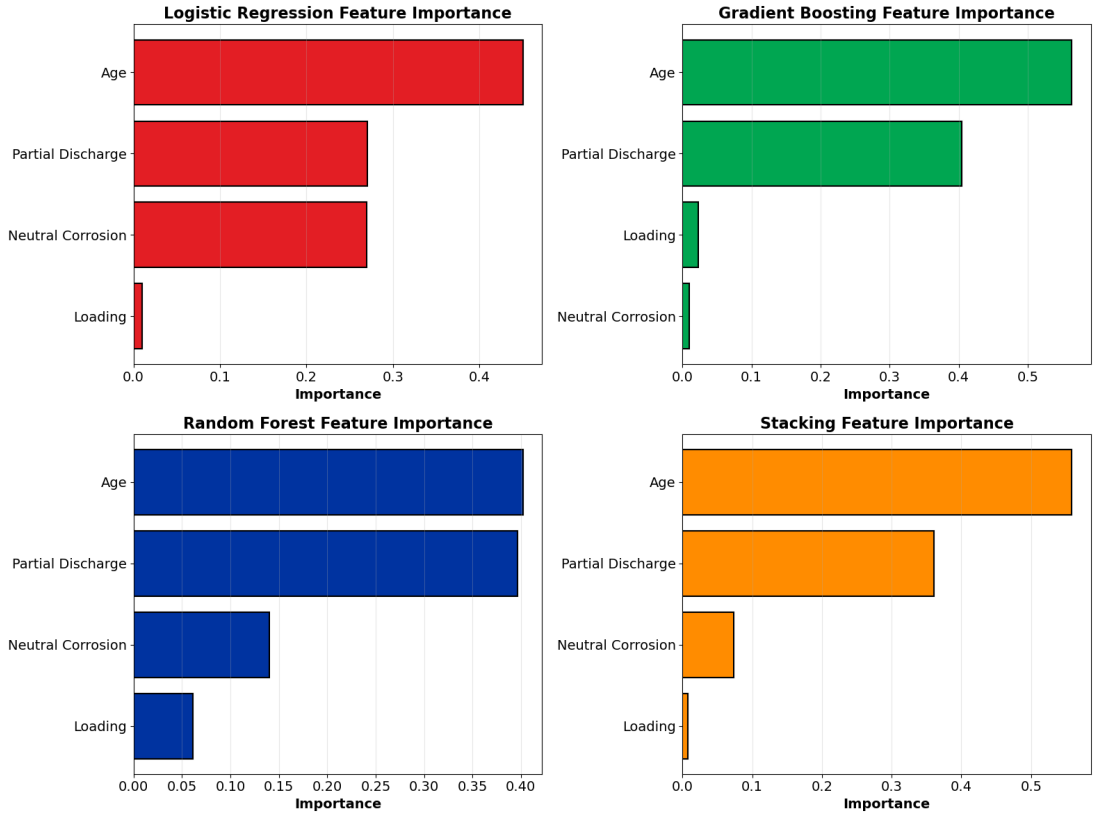

Figure 10. Feature importance bars for each individual model.

This Figure 11 and Table 4-2 aggregates feature importance into a consensus ranking, reducing dependence on any single algorithm's bias. Age and Partial Discharge dominate the average importance values (0.472 and 0.357), followed by Neutral Corrosion (0.140) and Loading (0.031).

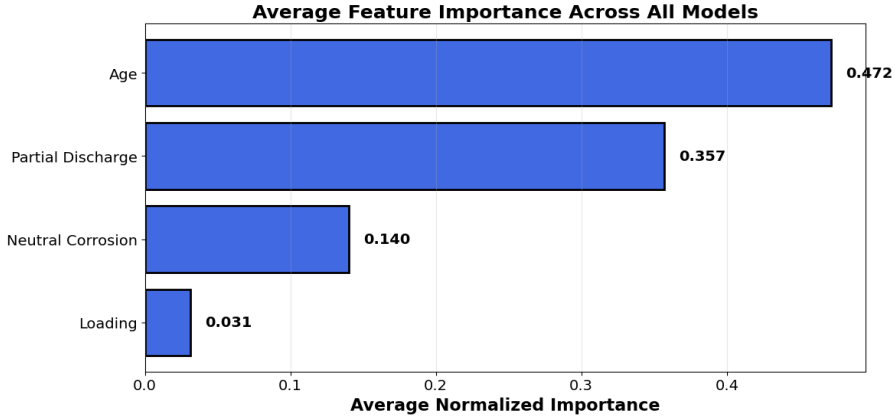

Figure 11. Average normalized importance across all models.

The result is consistent with the dataset's physical interpretation: aging and partial discharge are tightly linked to insulation degradation, corrosion adds secondary information on metallic shield/neutral condition, and loading varies operationally without consistently indicating deterioration in a snapshot. By summarizing across models, the plot supports robust feature prioritization for utilities and provides an interpretable justification for why the ensemble's decision logic aligns with domain expectations.

Table 4-2. Feature importance ranking from ensemble models

Feature	Importance
Age	0.472
Partial_Discharge	0.357
Neutral_Corrosion	0.140
Loading	0.031

The mean absolute SHAP plot in Figure 12 summarizes how strongly each input contributes to model output magnitude, broken down by class. Two features clearly have the largest average impacts across Good, Medium, and Poor, while the remaining features contribute much less. This pattern matches the feature-importance rankings where Age and Partial Discharge dominate predictive power, indicating that global explanations are consistent with model-level importance measures. The class-colored stacking also shows that the same dominant predictors influence multiple classes rather than being class-specific. Such alignment strengthens trust: the model's decisions are driven by stable degradation indicators rather than unstable, low-signal variables, improving interpretability.

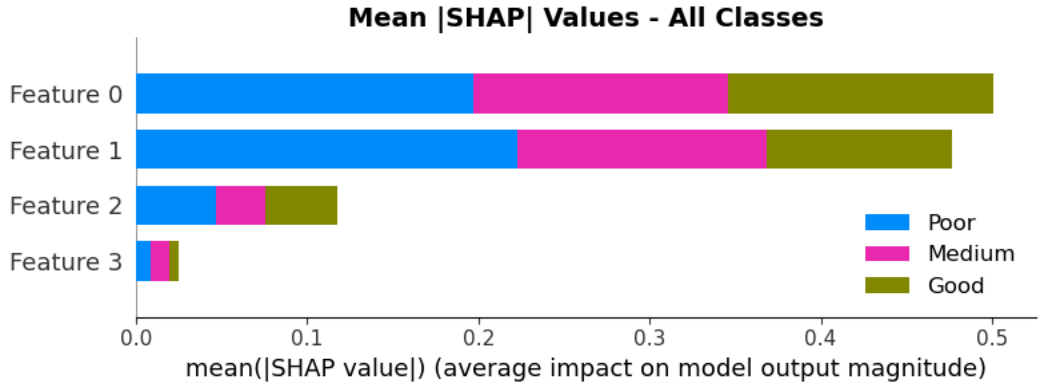

Figure 12. Global SHAP importance across condition classes.

The three beeswarm panels in Figure 13 show how feature values shift predictions within each class by displaying SHAP value distributions. Wide horizontal spreads indicate features that drive greater changes in predicted probability, while color gradients reveal whether high values push predictions toward or away from the class. The Good panel generally shows the opposite sign pattern compared with the Poor panel for the most influential features, reflecting the monotonic deterioration pathway: higher degradation indicators reduce Good likelihood and increase Poor likelihood. Medium exhibits mixed effects, consistent with its transitional nature and overlap with adjacent classes. These plots explain why Medium recall is lower in Table 4-1: many observations sit near the decision boundary, where small feature changes can flip the class.

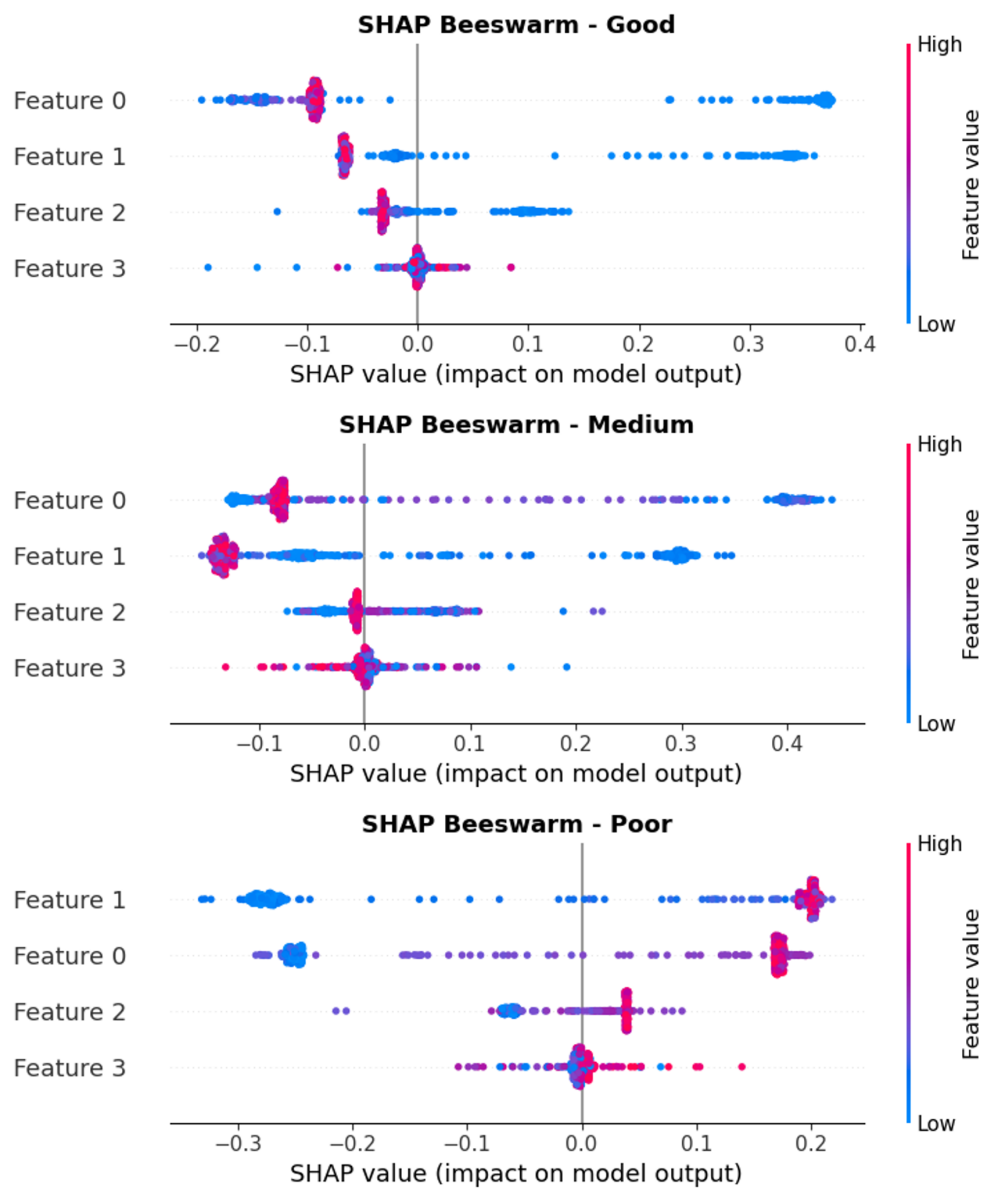

Figure 13. SHAP beeswarm plots for each visual condition class.

The dependence plots in Figure 15 highlight nonlinear response patterns for the Poor class. For the most influential predictors, SHAP values change sharply over a narrow feature range and then saturate, indicating threshold-like behavior where crossing a degradation level rapidly increases Poor probability. Neutral Corrosion shows a weaker, more scattered relationship, suggesting partial redundancy with the primary predictors. Loading exhibits near-flat SHAP trends with scattered points, consistent with low information content and higher noise relative to degradation variables. Interaction coloring suggests that operational factors may modulate effects slightly but do not dominate classification. These shapes help explain strong Poor recall in Table 4-1: once key predictors pass a threshold, the model becomes highly confident, reducing misclassification of severely degraded segments. Poor condition is typically the most critical/high-risk outcome in maintenance prioritization, so it gets the interpretability focus.

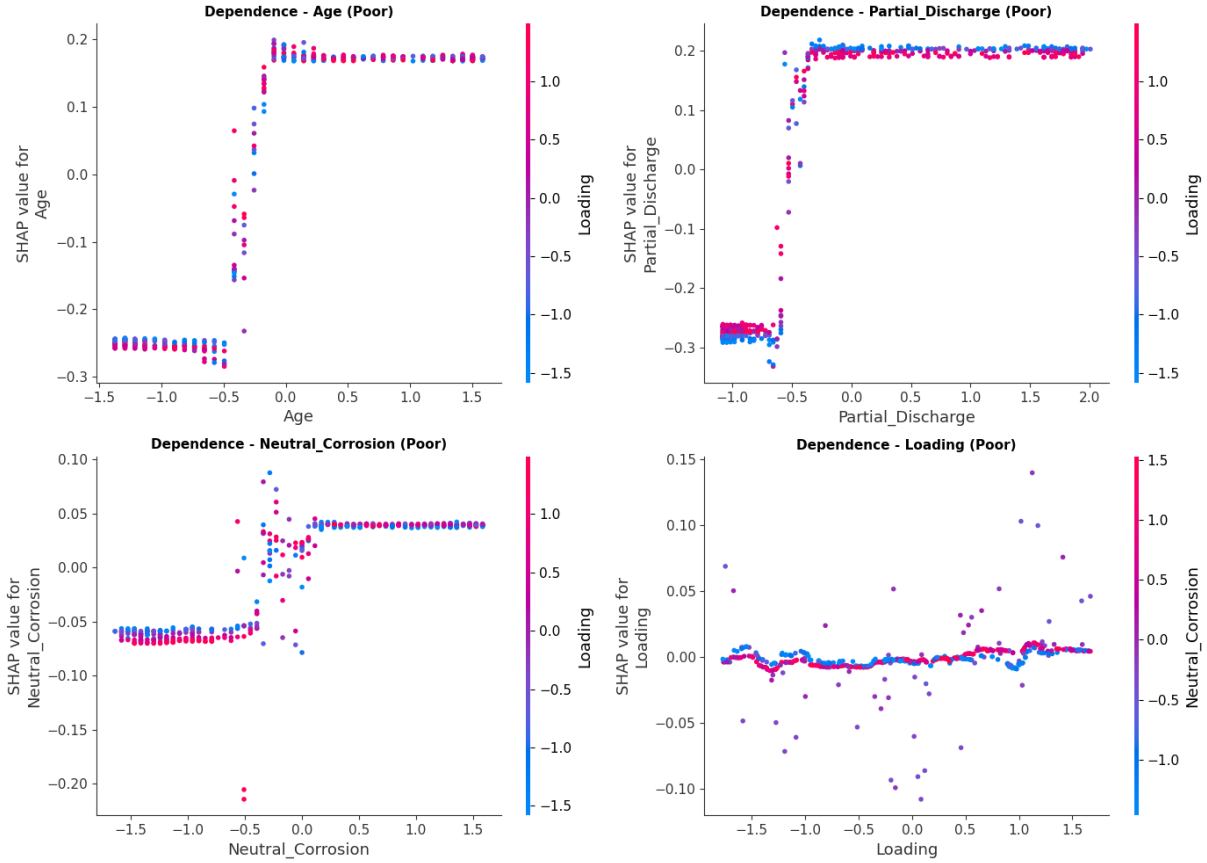

Figure 14. Nonlinear feature thresholds shaping prioritization classification.

The force plot in Figure 15 decomposes an individual prediction into additive feature contributions relative to a baseline expectation. Features pushing the output toward a higher Poor probability appear as strong directional contributions, while counteracting features pull in the opposite direction. The visualization shows that the prediction is primarily driven by the same dominant degradation indicators highlighted by global importance, with smaller adjustments from secondary variables. This consistency between local and global explanations supports interpretability: the model does not rely on unusual, case-specific quirks to classify Poor segments. Instead, it follows stable decision logic grounded in degradation signatures. Such instance-level explanations are useful operationally because they justify why a particular cable segment is flagged, supporting transparent prioritization for inspection or replacement.

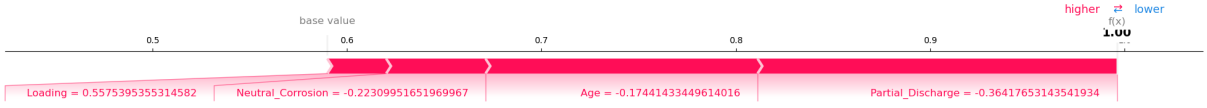

Figure 15. Local SHAP contributions shifting prediction probability.

The waterfall plot in Figure 16 presents the same local explanation as a cumulative additive path from the expected value to the final prediction. Larger bars indicate features with the greatest influence on the Poor probability for this specific sample, while smaller bars represent marginal adjustments. The pattern typically shows the strongest contributions from the primary degradation indicators, with minor influence from Loading—consistent with the low average importance of loading observed in Table 4-2 and the dependence plots. This coherence across interpretability views is important: it demonstrates that high-confidence Poor predictions arise from strong degradation signatures rather than noise. For reporting, the waterfall is particularly

effective because it provides an intuitive "reason chain" that can interpret without ML specialization.

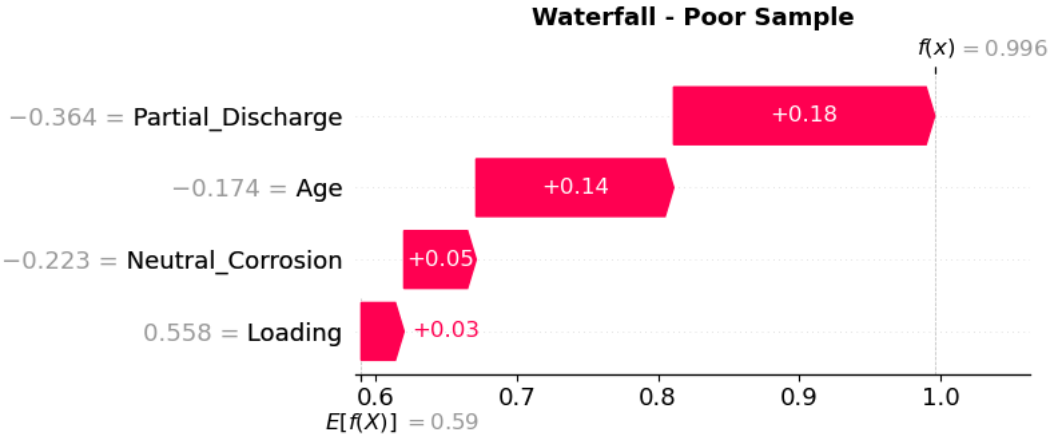

Figure 16. Additive feature contributions from baseline to output.

The four confusion matrices in Figure 17 reveal where each model makes mistakes across Good, Medium, and Poor conditions. Errors concentrate in adjacent-class confusions (Good↔Medium and Medium↔Poor), reflecting the transitional nature of Medium and the overlap in feature space. Poor is rarely misclassified as Good, indicating clear separation for severely degraded assets. The stacking matrix shows the fewest critical misclassifications and slightly improved diagonal dominance, aligning with its highest overall accuracy in Table 4-1. The counts also reflect class imbalance (Poor has the largest support), so improvements in Medium classification are especially valuable even when overall accuracy differences appear small. This figure provides an operational view of risk: it highlights the specific boundary where misprioritization is most likely.

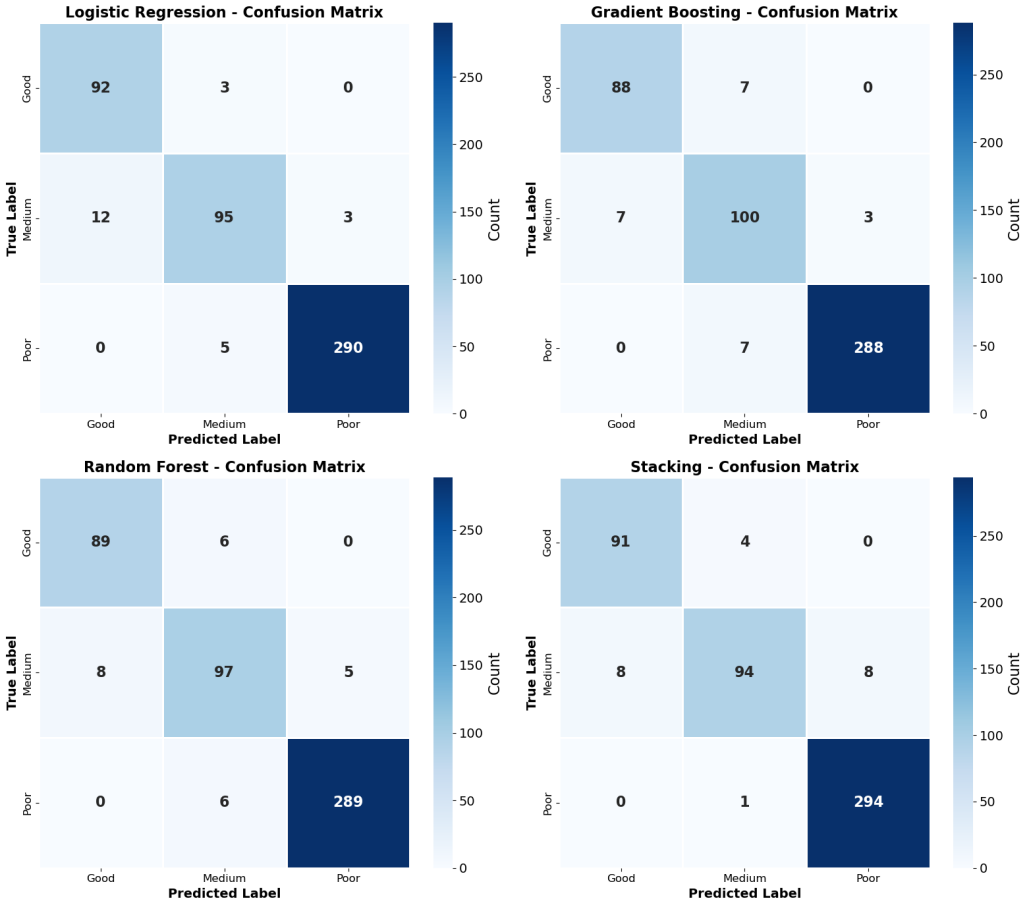

Figure 17. Confusion matrices for all models and condition classes.

Overall, results demonstrate that the proposed stacking ensemble framework delivers high and consistent predictive performance for three-class visual condition assessment of underground XLPE cables. Exploratory analyses show a strong coupled degradation structure among Age, Partial Discharge, and Neutral Corrosion, while Loading remains largely independent, a pattern confirmed by both correlation analysis and low importance rankings. Feature-importance results (Table 4-2) identify Age and Partial Discharge as primary drivers, with Neutral Corrosion adding secondary discrimination and Loading contributing minimally. Classification results (Table 4-1) show all models achieving strong performance (accuracy 0.95–0.96), with the stacking ensemble providing the best overall accuracy and weighted F1. These findings motivate a deeper interpretation of why the ensemble improves robustness and how the approach generalizes to broader utility settings, as discussed next.

5 DISCUSSION

The results show that a stacking ensemble can achieve robust multi-class discrimination on field-inspection tabular data when predictors encode physically meaningful degradation signals: the ensemble attains 0.96 accuracy with strong class-wise performance, including Poor F1 ≈ 0.98, while feature importance and SHAP-style explanations consistently emphasize Age and Partial Discharge as dominant drivers. These findings align with prior work highlighting insulation aging and discharge activity as key diagnostics, including neural-network aging prediction studies (e.g., Boukezzi & Boubakeur, 2013) [44] and PD classification surveys (e.g., Kumar et al., 2024) [46], while the strong separability of Poor-condition assets echoes simulated fault-classification results (e.g., Said et al., 2022) [48]. Several limitations should be noted: high collinearity among Age, Partial Discharge, and Neutral Corrosion may inflate separability; class imbalance can mask boundary errors for Medium; results rely on a single asset-level dataset with a 500-sample test split; and the snapshot features do not capture time-series degradation dynamics.

6 CONCLUSION

This study addressed underground 15-kV XLPE cable condition assessment by developing a data-driven stacking ensemble using a real-world asset-level inspection dataset. The framework combined Logistic Regression, Gradient Boosting, and Random Forest within a stacking architecture to predict visual condition classes, supported by exploratory analysis, feature standardization, and interpretability tools. Results showed consistently high performance, with the stacking ensemble achieving the best overall accuracy and weighted F1. Feature importance identified Age and Partial Discharge as dominant drivers, with Neutral Corrosion secondary and Loading minimal. Limitations include class imbalance, predictor collinearity, and the need for broader validation, but the approach provides an interpretable basis for risk-informed maintenance prioritization.

7 RECOMMENDATION

Future work should improve generalizability by validating the stacking framework on multi-utility, multi-region datasets and adding temporal features (e.g., PD trends, seasonal loading) to capture degradation dynamics. Model reliability can be strengthened with uncertainty quantification (calibrated probabilities, conformal/Bayesian ensembles) and drift monitoring for long-term deployment. For scalability, advanced boosting libraries such as LightGBM/CatBoost and sequence models (LSTM/Transformers) can be explored. For practical adoption, integrate predictions and explanations into utility platforms such as IBM

Maximo, Oracle Utilities WAM, SAP Intelligent Asset Management, and GIS via ArcGIS Utility Network, complemented by DNV Cascade, Doble Calisto monitoring, and Sentient Energy Ample underground analytics.

8 REFERENCES

[1] E. Diaz-Dorado, J. Cidras, and E. Miguez, "Application of evolutionary algorithms for the planning of urban distribution networks of medium voltage," *IEEE Transactions on Power Systems*, vol. 17, no. 3, pp. 879–884, Aug. 2002, doi: 10.1109/TPWRS.2002.800975.

[2] Y. Murata *et al.*, "Development of high voltage DC-XLPE cable system," *SEI Tech. Rev*, vol. 101, pp. 55–62, 2013.

[3] L. Yang, J. Fan, Y. Liu, E. Li, J. Peng, and Z. Liang, "A review on state-of-the-art power line inspection techniques," *IEEE Trans. Instrum. Meas.*, vol. 69, no. 12, pp. 9350–9365, 2020.

[4] A. Khojaste, J. Pearce, D. P. de Farias, G. Pritchard, and G. Zakeri, "Risk-Averse Markov Decision Processes: Applications to Electricity Grid and Reservoir Management," *arXiv preprint arXiv:2601.02207*, 2026.

[5] G. Liu *et al.*, "Power cables for triboelectric nanogenerator networks for large-scale blue energy harvesting," *Nano Energy*, vol. 75, p. 104975, 2020.

[6] Y. Mousavi *et al.*, "Cyber-Resilient Data-Driven Event-Triggered Secure Control for Autonomous Vehicles Under False Data Injection Attacks," *arXiv preprint arXiv:2511.15925*, 2025.

[7] L. Lucantoni, S. Antomarioni, F. E. Ciarapica, and M. Bevilacqua, "A data-driven framework for supporting the total productive maintenance strategy," *Expert Syst. Appl.*, vol. 268, p. 126283, Apr. 2025, doi: 10.1016/j.eswa.2024.126283.

[8] C.-M. Jung, P. Ray, and S. R. Salkuti, "Asset management and maintenance: a smart grid perspective," *International Journal of Electrical and Computer Engineering (IJECE)*, vol. 9, no. 5, p. 3391, Oct. 2019, doi: 10.11591/ijece.v9i5.pp3391-3398.

[9] P. Beigvand, M. Najafi, V. Kaushal, A. Mohammadi, W. Elledge, and B. Kaynak, "Assessing the Environmental and Occupational Health Implications of Styrene Emissions in Cured-In-Place Pipe (CIPP) Rehabilitation: A Multi-Site Analysis of Installation Practices," *Int. J. Environ. Res. Public Health*, vol. 22, no. 10, p. 1543, Oct. 2025, doi: 10.3390/ijerph22101543.

[10] L. Rojas, A. Peña, and J. Garcia, "AI-Driven Predictive Maintenance in Mining: A Systematic Literature Review on Fault Detection, Digital Twins, and Intelligent Asset Management," *Applied Sciences*, vol. 15, no. 6, p. 3337, Mar. 2025, doi: 10.3390/app15063337.

[11] S. Mirzaei, S. Bunt, and S. M. Bogus, "A human-centered approach to reframing job satisfaction in the BIM-enabled construction industry," *arXiv preprint arXiv:2512.20584*, 2025.

[12] P. Beigvand, M. Najafi, V. Kaushal, W. Elledge, B. Kaynak, and A. Mohammadi, "A Comprehensive Analysis of Styrene Emissions in Cured-in-Place Pipe Installations Using Polyester (Styrene-Based) Resin Liners across Multiple Jobsites," in *Pipelines 2025*, Reston, VA: American Society of Civil Engineers, Aug. 2025, pp. 267–277. doi: 10.1061/9780784486375.031.

[13] D. Cui *et al.*, "Enhancing Short-Term Electricity Forecasting with Advanced Machine Learning Techniques," *Journal of Electrical Engineering & Technology*, vol. 21, no. 1, pp. 147–187, Jan. 2026, doi: 10.1007/s42835-025-02430-z.

[14] Y. Liu, J. Cao, C. Liu, K. Ding, and L. Jin, "Datasets for large language models: a comprehensive survey," *Artif. Intell. Rev.*, vol. 58, no. 12, p. 403, Oct. 2025, doi: 10.1007/s10462-025-11403-7.

[15] J. Liu, S. Yuan, B. Luo, B. Biondi, and H. Y. Noh, "Turning Telecommunication Fiber-Optic Cables into Distributed Acoustic Sensors for Vibration-Based Bridge Health Monitoring," *Struct. Control Health Monit.*, vol. 2023, pp. 1–14, Apr. 2023, doi: 10.1155/2023/3902306.

[16] F. Aminifar, M. Abedini, T. Amraee, P. Jafarian, M. H. Samimi, and M. Shahidehpour, "A review of power system protection and asset management with machine learning techniques," *Energy Systems*, vol. 13, no. 4, pp. 855–892, Nov. 2022, doi: 10.1007/s12667-021-00448-6.

[17] S. Eslamdoust, J. Jeong, J. H. Lee, Y. Dai, and B. Lyu, "Job Stress, Emotional Exhaustion, and Work-Family Conflict: A Moderated Mediation Model," *Journal of Chinese Human Resources Management*, vol. 17, no. 1, pp. 193–208, 2026.

[18] L. Bellani *et al.*, "A reliability-centered methodology for identifying renovation actions for improving resilience against heat waves in power distribution grids," *International Journal of Electrical Power & Energy Systems*, vol. 137, p. 107813, May 2022, doi: 10.1016/j.ijepes.2021.107813.

[19] M. M. Ghahfarokhi, H. Jahantigh, A. Asadi, and A. Heydarnoori, "Integrating Code Metrics into Automated Documentation Generation for Computational Notebooks," *arXiv preprint arXiv:2602.08133*, 2026.

[20] S. Mashhadi, "The Universal Proxy Rule, Proxy Contests, and Shareholder Voting," *Proxy Contests, and Shareholder Voting (January 09, 2026)*, 2026.

[21] A. Khosravani, A. Hosseinpour, A. Akhavan, M. Keshani, and A. Heydarnoori, "LIA: Supervised Fine-Tuning of Large Language Models for Automatic Issue Assignment," *arXiv preprint arXiv:2601.01780*, 2026.

[22] S. Mashhadi, "The First Chicago Valuation Method," 2023, pp. 159–181. doi: 10.1007/978-3-031-35291-1_8.

[23] A. Zien, N. Krämer, S. Sonnenburg, and G. Rätsch, "The Feature Importance Ranking Measure," *Lecture Notes in Computer Science (including subseries Lecture Notes in Artificial Intelligence and Lecture Notes in Bioinformatics)*, vol. 5782 LNAI, no. PART 2, pp. 694–709, 2009, doi: 10.1007/978-3-642-04174-7_45.

[24] X. Wu *et al.*, "Design and behavior of 160 m-tall post-tensioned precast concrete-steel hybrid wind turbine tower," *Steel and Composite Structures*, vol. 44, no. 3, pp. 407–421, 2022.

[25] P. Niu *et al.*, "Multi-objective optimal tolerance allocation design of machine tool based on NSGA-II algorithm and thermal characteristic analysis," *Proc. Inst. Mech. Eng. B J. Eng. Manuf.*, vol. 240, no. 1–2, pp. 244–257, Jan. 2026, doi: 10.1177/09544054241310330.

[26] V. Nasteski, "An overview of the supervised machine learning methods," *HORIZONS.B*, vol. 4, pp. 51–62, Dec. 2017, doi: 10.20544/HORIZONS.B.04.1.17.P05.

[27] H. Irani and V. Metsis, "Positional encoding in transformer-based time series models: A survey," *arXiv preprint arXiv:2502.12370*, 2025.

[28] A. Shekofteh and R. A. Chou, "Improved Achievable Rate for Single-Server SPIR over Binary Erasure Channels," in *2025 61st Allerton Conference on Communication, Control, and Computing Proceedings*, Allerton Conference on Communication, Control, and Computing, 2025.

[29] N. P. Bhatta, S. Al Majmaie, and F. Amsaad, "Securing IoT/Edge Computing Infrastructure for Smart Agriculture: Challenges and Solutions," in *2025 1st International Conference on Secure IoT, Assured and Trusted Computing (SATC)*, IEEE, Feb. 2025, pp. 1–5. doi: 10.1109/SATC65530.2025.11136873.

[30] H. Henderi, T. Wahyuningsih, and E. Rahwanto, "Comparison of Min-Max normalization and Z-Score Normalization in the K-nearest neighbor (kNN) Algorithm to Test the Accuracy of Types of Breast Cancer," *International Journal of Informatics and Information Systems*, vol. 4, no. 1, pp. 13–20, Mar. 2021, Accessed: Jul. 11, 2025. [Online]. Available: https://ijiis.org/index.php/IJIIS/article/view/73

[31] A. Shekofteh and R. A. Chou, "Single-server SPIR over binary erasure channels: Benefits of noisy side information," in *2025 61st Allerton Conference on Communication, Control, and Computing Proceedings*, Allerton Conference on Communication, Control, and Computing, 2025.

[32] B. Kiafar, S. Daher, A. Ahmmed, and R. L. Barmaki, “A Quantitative Ethnographic Analysis of Caregiver Competencies and Engagement in Augmented Reality Geriatric Simulation,” 2026, pp. 321–335. doi: 10.1007/978-3-032-12229-2_21.

[33] B. G. Damirchi, S. Jahromi, G. Sdoukopoulou, S. Shahdadian, and C. Papadelis, “Induction of Gamma Oscillations via Transcranial Temporal Interference Stimulation: A Human Head Phantom Study,” in *2025 47th Annual International Conference of the IEEE Engineering in Medicine and Biology Society (EMBC)*, IEEE, Jul. 2025, pp. 1–4. doi: 10.1109/EMBC58623.2025.11253435.

[34] M. Sadiq *et al.*, “MXene-montmorillonite nanocomposites-based scaffold sensors for early pancreatic cancer diagnosis,” *Cancer Plus*, vol. 6, no. 3, p. 3793, Oct. 2024, doi: 10.36922/cp.3793.

[35] B. G. Damirchi, S. Jahromi, A. Vaysi, H. Partamian, S. Shahdadian, and C. Papadelis, “Non-Invasive Deep Brain Stimulation with Temporal Interference: Multimodal Validation with a 3D-Printed Pediatric Head Phantom,” Oct. 21, 2025. doi: 10.36227/techrxiv.176101827.72413327/v1.

[36] C. Lin *et al.*, “Multi-model ensemble learning for battery state-of-health estimation: Recent advances and perspectives,” *Journal of Energy Chemistry*, vol. 100, pp. 739–759, Jan. 2025, doi: 10.1016/j.jechem.2024.09.021.

[37] J. M. Hilbe, “Logistic Regression,” in *International Encyclopedia of Statistical Science*, Berlin, Heidelberg: Springer Berlin Heidelberg, 2025, pp. 1386–1390. doi: 10.1007/978-3-662-69359-9_333.

[38] G. Grekousis, “Geographical-XGBoost: a new ensemble model for spatially local regression based on gradient-boosted trees,” *J. Geogr. Syst.*, vol. 27, no. 2, pp. 169–195, Apr. 2025, doi: 10.1007/s10109-025-00465-4.

[39] C. Chen, J. Liang, W. Sun, G. Yang, and X. Meng, “An automatically recursive feature elimination method based on threshold decision in random forest classification,” *Geo-spatial Information Science*, vol. 28, no. 4, pp. 1494–1519, Jul. 2025, doi: 10.1080/10095020.2024.2387457.

[40] H. Irani, Y. Ghahremani, A. Kermani, and V. Metsis, “Time Series Embedding Methods for Classification Tasks: A Review,” *Expert Syst.*, vol. 42, no. 11, Nov. 2025, doi: 10.1111/exsy.70148.

[41] Y. Li, Q. Chen, G. Strbac, K. Hur, and C. Kang, “Active Distribution Network Expansion Planning With Dynamic Thermal Rating of Underground Cables and Transformers,” *IEEE Trans. Smart Grid*, vol. 15, no. 1, pp. 218–232, Jan. 2024, doi: 10.1109/TSG.2023.3266782.

[42] Y. Song *et al.*, “Online multi-parameter sensing and condition assessment technology for power cables: A review,” *Electric Power Systems Research*, vol. 210, p. 108140, Sep. 2022, doi: 10.1016/j.epsr.2022.108140.

[43] J. J. Bush, R. J. Flask, and I. V Raleigh Benton Stelle, “Intelligent monitoring and testing system for cable network,” Jan. 21, 2025, *Google Patents*.

[44] L. Boukezzi and A. Boubakeur, “Prediction of mechanical properties of XLPE cable insulation under thermal aging: Neural network approach,” *IEEE Transactions on Dielectrics and Electrical Insulation*, vol. 20, no. 6, pp. 2125–2134, 2013, doi: 10.1109/TDEI.2013.6678861.

[45] Y. Huo, G. Prasad, L. Lampe, and V. C. M. Leung, “Advanced Smart Grid Monitoring: Intelligent Cable Diagnostics using Neural Networks,” in *2020 IEEE International Symposium on Power Line Communications and its Applications (ISPLC)*, IEEE, May 2020, pp. 1–6. doi: 10.1109/ISPLC48789.2020.9115403.

[46] H. ; Kumar, M. ; Shafiq, K. ; Kauhaniemi, and M. A. Elmusrati, “A Review on the Classification of Partial Discharges in Medium-Voltage Cables: Detection, Feature Extraction, Artificial Intelligence-Based Classification, and Optimization Techniques,” *Energies 2024, Vol. 17, Page 1142*, vol. 17, no. 5, p. 1142, Feb. 2024, doi: 10.3390/EN17051142.

[47] S. Li, B. Cao, J. Li, Y. Cui, Y. Kang, and G. Wu, "Review of condition monitoring and defect inspection methods for composited cable terminals," *High Voltage*, vol. 8, no. 3, pp. 431–444, Jun. 2023, doi: 10.1049/hve2.12318.

[48] A. Said, S. Hashima, M. M. Fouda, and M. H. Saad, "Deep Learning-Based Fault Classification and Location for Underground Power Cable ," *IEEE Access*, vol. 10, pp. 70126–70142, 2022, doi: 10.1109/ACCESS.2022.3187026.

[49] J. Kong, K. Zhou, Y. Chen, P. Meng, Y. Li, and X. Ren, "A Novel Condition Assessment Method for Corrugated Aluminum Sheathed XLPE Cables Based on Evolved Gas Analysis," *IEEE Transactions on Dielectrics and Electrical Insulation*, vol. 30, no. 2, pp. 883–891, Apr. 2023, doi: 10.1109/TDEI.2022.3228213.

[50] S. Uriarte, H. Baier-Fuentes, J. Espinoza-Benavides, and W. Inzunza-Mendoza, "Artificial intelligence technologies and entrepreneurship: a hybrid literature review," *Review of Managerial Science*, vol. 20, no. 1, pp. 251–299, Jan. 2026, doi: 10.1007/s11846-025-00839-4.

[51] E. Ip *et al.*, "Distributed fiber sensor network using telecom cables as sensing media: technology advancements and applications [Invited]," *Journal of Optical Communications and Networking*, vol. 14, no. 1, p. A61, Jan. 2022, doi: 10.1364/JOCN.439175.

[52] J. Feng, K. Gao, W. Gao, Y. Liao, and G. Wu, "Machine learning-based bridge cable damage detection under stochastic effects of corrosion and fire," *Eng. Struct.*, vol. 264, p. 114421, Aug. 2022, doi: 10.1016/j.engstruct.2022.114421.

[53] J. Kufel *et al.*, "What Is Machine Learning, Artificial Neural Networks and Deep Learning?—Examples of Practical Applications in Medicine," *Diagnostics*, vol. 13, no. 15, p. 2582, Aug. 2023, doi: 10.3390/diagnostics13152582.

[54] UtilityAnalytics, "15KV XLPE Underground Cable Inspection Dataset." Accessed: Feb. 25, 2026. [Online]. Available: https://www.kaggle.com/datasets/utilityanalytics/utility-underground-cable-dataset1

[55] H. Alimohammadi and S. Nancy Chen, "Performance evaluation of outlier detection techniques in production timeseries: A systematic review and meta-analysis," *Expert Syst. Appl.*, vol. 191, p. 116371, Apr. 2022, doi: 10.1016/j.eswa.2021.116371.

[56] Z. Šverko, M. Vrankić, S. Vlahinić, and P. Rogelj, "Complex Pearson Correlation Coefficient for EEG Connectivity Analysis," *Sensors*, vol. 22, no. 4, p. 1477, Feb. 2022, doi: 10.3390/s22041477.

[57] K. Cabello-Solorzano, I. Ortigosa de Araujo, M. Peña, L. Correia, and A. J. Tallón-Ballesteros, "The Impact of Data Normalization on the Accuracy of Machine Learning Algorithms: A Comparative Analysis," 2023, pp. 344–353. doi: 10.1007/978-3-031-42536-3_33.

[58] R. A. Disha and S. Waheed, "Performance analysis of machine learning models for intrusion detection system using Gini Impurity-based Weighted Random Forest (GIWRF) feature selection technique," *Cybersecurity*, vol. 5, no. 1, p. 1, Dec. 2022, doi: 10.1186/s42400-021-00103-8.

[59] X. He *et al.*, "Federated Continuous Learning Based on Stacked Broad Learning System Assisted by Digital Twin Networks: An Incremental Learning Approach for Intrusion Detection in UAV Networks," *IEEE Internet Things J.*, vol. 10, no. 22, pp. 19825–19838, Nov. 2023, doi: 10.1109/JIOT.2023.3282648.

[60] J. H. Steiger, "Tests for comparing elements of a correlation matrix.," *Psychol. Bull.*, vol. 87, no. 2, pp. 245–251, Mar. 1980, doi: 10.1037/0033-2909.87.2.245.

[61] D. Silver and Xin Wang, "Tracking and visualizing turbulent 3D features," *IEEE Trans. Vis. Comput. Graph.*, vol. 3, no. 2, pp. 129–141, 1997, doi: 10.1109/2945.597796.